

1 Presenting multivariate statistical 2 protocols in R using Roman wine 3 amphorae productions in Catalonia, 4 Spain

5

6 *Corresponding author*

7 Andreas Angourakis¹

8 andros.spica@gmail.com ; andreas.angourakis@ub.edu

9 *Co-authors*

10 Verònica Martínez Ferreras¹, Alexis Torrano², Josep M. Gurt Esparraguera¹

11 ¹ERAAUB, Department of Prehistory, Ancient History and Archaeology, University of
12 Barcelona, C/Montalegre, 6, 08001 Barcelona, Spain.

13 ²BSC/CNS, Barcelona Supercomputing Center/Centro Nacional de Supercomputación.
14 Carrer de Jordi Girona, 29-31, 08034 Barcelona, Spain.

15 *Highlights*

- 16 • Geochemical and petrographic data often present different patterns in ceramics.
- 17 • We define four protocols for applying multivariate statistics in ceramics.
- 18 • We offer two R packages for applying these protocols.
- 19 • We demonstrate their performance using a dataset of Roman wine amphorae.
- 20 • The fourth protocol is the most effective in evidencing the provenance of materials.

21 *Abstract*

22 Several analytic techniques can provide data for characterizing archaeological ceramics. These
23 data sources are not alternative but rather complementary to each other. They report on
24 different aspects of ceramics concerning the origin of raw materials and the technological
25 processes involved. However, when studies integrate more than one data source, they often
26 do it through textual description and argument, not through a combined statistical analysis.

27 We aim to help to overcome this situation by presenting four protocols for exploring data on
28 archaeological ceramics. These protocols cover four different paths when interrogating
29 ceramic samples. Protocol 1 aims to assist the definition of chemical reference groups using
30 geochemical compositions, for instance, given by X-ray fluorescence analysis (WD-XRF).
31 Protocol 2 focuses on fabric groups using petrographic examinations, such as in thin-section
32 optical microscopy. Protocol 3 offers a hybrid assessment of provenance, using the integral

33 sum of the two data sources. Last, Protocol 4 consists of the same approach as Protocol 3 but
34 using geochemical data and a selection of petrographic variables that are considered indicative
35 of the origin of raw materials and independent of human factors. We demonstrate their
36 performance by applying them to a well-studied Roman wine amphorae dataset from
37 Catalonia, NE Spain, and contextualising the results. Through a comparison of the results
38 produced by these protocols, we restate the conclusion of Baxter et al. (2008) that a ‘mixed
39 mode’ approach is preferable to analysing data from different sources separately. Moreover,
40 we argue that treating geochemical data as compositional and petrographic semi-quantitative
41 observations as ordinal variables, when calculating dissimilarity, offers a more complete image
42 of ceramic materials.

43 The protocols are the synthetic product of several multivariate statistical methods developed
44 for similar purposes in other disciplines, such as geology and ecology. To allow future users to
45 replicate our analysis and apply the protocols, we published online two R packages containing
46 all necessary procedures, from data cleaning to plotting. We also offer in the appendices a
47 tutorial and the example scripts.

48 *Keywords*

49 Ceramics; archaeometric characterization; geochemical composition; petrography;
50 multivariate statistics; R; Roman amphorae

51

52 *Abbreviations*

53 alr, clr, ilr: additive, centered, isometric log-ratio
54 CA: correspondence analysis
55 CHEM : geochemical data
56 FGs: fabric groups
57 IND: tag for site-wise outliers (e.g., FEU-IND2 is the second outlier in the Fenals)
58 NI: neighbour interchange approach to measure dissimilarity in ordinal variables
59 NMDS: non-metric multidimensional scaling
60 PCA : principal components analysis
61 PCoA : principal coordinates analysis
62 PETRO: mineralogical and petrographic data
63 PGs: provenance groups
64 RGs: chemical reference groups
65 RPCA: robust principal component analysis
66 RRD: relative rank difference approach to measure dissimilarity in ordinal variables
67 WD-XRF: X-ray fluorescence analysis
68 Amphorae formal types:
69 D1: Dressel 1
70 D2/4: Dressel 2/4
71 D7/11: Dressel 7/11
72 L2: Lamboglia 2
73 Ob.74: Oberaden 74
74 P1: Pascual 1
75 T1, T3: Tarraconense 1 and 3
76

77

78 1. Introduction

79 Pottery provenance and technology are well-studied fields in archaeology since they
80 largely contribute to the economic, social and cultural reconstruction of past societies.
81 The examination of the composition and the morphological and technical
82 characteristics of pottery vessels allows making many inferences about them, their
83 creators and users. Typically, we are capable of assessing their provenance and
84 performance characteristics, which informs on the technological skills and traditions
85 involved in their manufacture, trade relationships, the expectations of consumers, etc.
86 (Schiffer and Skibo, 1997, 1987; Sillar and Tite, 2000).

87 Archaeology is today conceptually and technically well equipped to address this
88 system, given enough evidence (Tite, 2008). Since the 1960s, the incorporation of
89 scientific methods in the study of ancient pottery has been a significant advance in the
90 fields of study. Provenance analysis is used to locate specific pottery designs and
91 technological patterns in particular places and periods, as well as trade relationships
92 between different areas. The investigation through thin-section optical microscopy
93 entails an in-depth study of the geological regions concerned. Provenance can also be
94 accurately established through chemical analysis, although reference databases of the
95 corresponding pottery productions and local raw materials are required. Through a
96 wide range of spectroscopic and microscopic methods, archaeologists can investigate
97 the technological processes involved in pottery manufacture (the procurement and
98 processing of raw materials, forming, finishing, firing, and surface treatments). When
99 approaching pottery artefacts from a long-term perspective, we can address the
100 evolution of pottery making and style, possibly discerning specific cultural and
101 technological patterns. However, contributions are often limited to a partial
102 characterization according to the technical and theoretical backgrounds of the
103 researchers involved. Usually, the plethora of possible analyses will not reach their
104 potential regarding results, if not sufficiently integrated with data obtained with other
105 methods, including qualitative and semi-quantitative data.

106 Despite the diversity of approaches in studying pottery artefacts, archaeologists should
107 be able to reverse-engineer most technological aspects related to pottery production
108 and use. The end goal of such analyses is to reconstruct the system entangling potters'
109 decisions and constraints—i.e., *chaîne opératoire* defined by Cresswell (1990)—which
110 have both universal and contextual components (Sillar and Tite, 2000).

111 To our knowledge, the clearest example of the integration of data on archaeological
112 ceramics is the work of Baxter et al. (2008). Their paper successfully illustrates the
113 benefits of combining petrographic and geochemical data to improve classifications
114 based on macroscopic features. Our contribution builds on their conclusions, as we
115 also aim to demonstrate the virtues and limitations of “mixed-mode” analyses. Based
116 on the Baxter et al. (2008) seminal experience, we explored different paths to achieve
117 integration. We focused on statistical methods developed in other disciplines
118 (Filzmoser et al., 2009; Pavoine et al., 2009; Podani, 1999), that exploit computational
119 resources while moving towards reproducible research (Gandrud, 2016; Marwick,
120 2017). Regarding the processing of geochemical data, we side with those authors that
121 have advocated for log-ratios (Aitchison, 1982; Buxeda i Garrigós, 1999; Martín-

122 Fernández et al., 2015; Pawlowsky-Glahn and Buccianti, 2011) rather than some form
123 of standardization (e.g., log-scaled). Though not favouring log-ratios, Baxter (2008)
124 summarized this debate with refreshing clarity, identifying arguments that are still valid
125 today.

126 We synthesize our explorations by presenting a multivariate methodology implemented
127 in R (R Core Team, 2015), which is an entirely free and open-source statistical
128 software widely used in academia. We published an R package online, *cerUB*
129 (Angourakis and Martínez Ferreras, 2017), containing the code required for applying
130 this methodology on comparable datasets. We encourage further extensions and
131 improvements by the community, as we were allowed to do so, particularly regarding
132 the contribution of Pavoine et al. (2009).

133 The greatest challenge for integration is that, while the geochemical composition is
134 strictly quantitative, both mineralogical and petrographic compositions often go through
135 qualitative assessments before any attempt of quantification, at least within
136 archaeological studies. However, we acknowledge that there are quantitative
137 approaches to petrographic (i.e., point-counting) and mineralogical (i.e., digital image)
138 analyses that are increasingly being used on archaeological ceramics (Quinn 2013).
139 Although beyond the scope of our current proposal, these analyses will be considered
140 for additional protocols in the future.

141 Once we designed a pottery database reflecting these and other aspects (section 2.2),
142 we explored separate datasets involving different working hypotheses (e.g.,
143 provenance diversity, technological change). After much exploration, we define four
144 statistical protocols of multivariate analysis to measure and represent dissimilarity
145 between individual ceramics (section 2.3). The first three address respectively the
146 geochemical composition (protocol 1), the petrographic characterization with data
147 inferred from the mineralogical and petrographic compositions (protocol 2), and both
148 data sources simultaneously (protocol 3). Protocol 4 differs from protocol 3 by selecting
149 variables considered indicative of provenance.

150 We apply each protocol on a collection of Roman wine amphorae to demonstrate their
151 performance in measuring and visualizing dissimilarity between archaeological
152 ceramics. The collection includes samples found in fifteen workshops in Catalonia, NE
153 Spain, and three shipwrecks sunk along the coast towards Narbonne, SE France
154 (section 2.1). Both workshop productions and amphorae from the ships' cargoes were
155 fully characterized in previous studies (Martínez Ferreras, 2014; Martínez Ferreras et
156 al., 2015, 2013).

157 Through this approach we expect (a) to provide the analyst with a straightforward
158 image of the pottery variability, thus aiding archaeological classification; and (b) to
159 facilitate the identification of the most relevant factors among variables, to guide future
160 finer analyses. Ultimately, we intend this methodology to be a useful tool for assessing
161 the context of pottery-making, as well as the transport of materials for trade or tribute
162 and the technological change among past societies.

163 **2. Material and methods**

164 **2.1. Archaeological materials**

165 The sample consists of a total of 236 Roman wine amphorae (Figure 1, Table 1): 175
 166 found in 15 workshops located in different production areas of the Catalan littoral and
 167 pre-littoral depressions, which initiated pottery activity at different times; and 61
 168 recovered in three shipwrecks along the coast towards Narbonne, France.

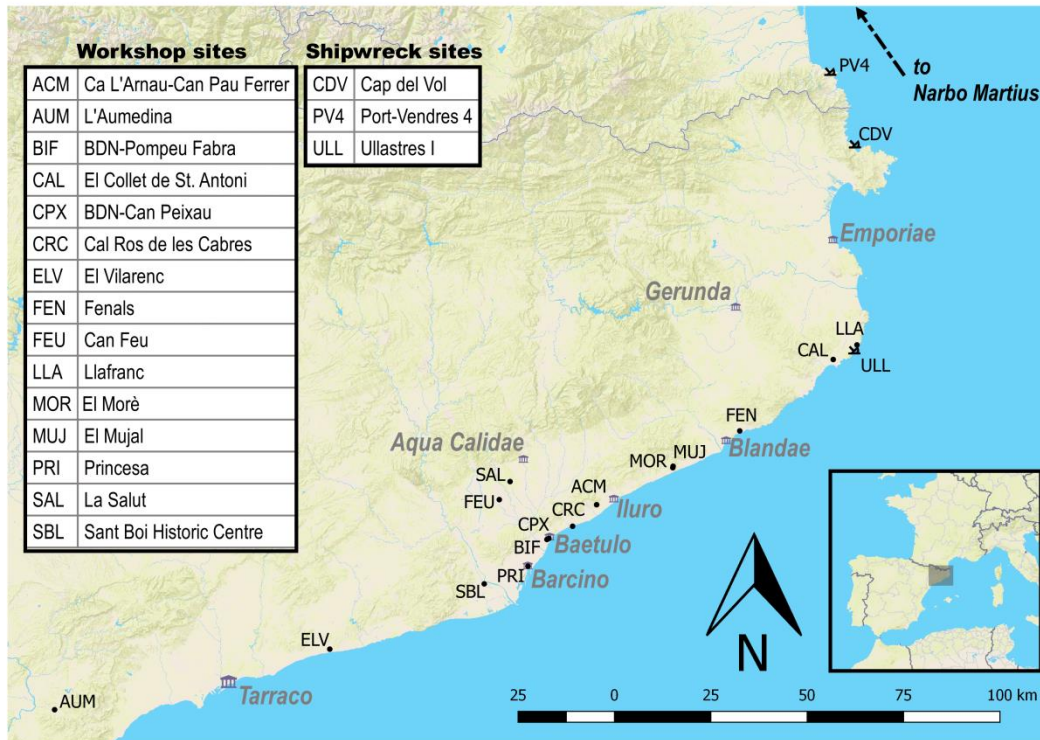


Figure 1. The location of the main Roman settlements in the Catalan coast (NE Spain), the fifteen amphora workshops and the three shipwrecks included in the analysis.

169 From c. 100 BC to 25 AD, the manufacture of amphorae in the region focused on wine
 170 production and export, feeding the maritime trade routes and reaching several port
 171 cities, such as *Narbo Martius* (Narbonne) in *Galia Narbonensis* (Martínez Ferreras,
 172 2015).

173 The collection includes several typological forms of transport amphorae corresponding
 174 to specific periods and production areas. The first amphora design consists of a copy of
 175 the Dressel 1 (D1) prototype which was by far the most common Italian amphora for
 176 wine trade in the western Mediterranean. It existed in the Laietan region (nowadays El
 177 Maresme) especially in a few workshops located around the Roman city of *Iluro*
 178 (Mataró) such as in ACM. Another isolated production of the D1 type has been
 179 identified at La Salut (SAL), located in the western pre-littoral area near the Ripoll River
 180 Basin. The area of *Iluro* was also the focus of the introduction in c. 50 BC of new
 181 variants of an amphora prototype called *Tarraconense 1* (T1), in sites such as ACM
 182 and MUJ. The workshops at ELV and SAL also produced other variants, which
 183 progressively replaced the D1 type.

Site	Location	Category	Chronology	Amphorae types
AUM Aumedina	Tivissa (Ribera d'Ebre)	Wine centre and pottery workshop	30 BC – 1 st c. AD	P1, D7/11, Ob.74
ELV El Vilarenc	Calafell (Baix Penedès)	<i>Villa</i> , wine centre and pottery workshop	40 BC – 50 AD	D1, T1, T3, P 1, Flat base
SBL Barri Antic	S. Boi Llobregat (Baix Llobregat)	<i>Villa</i> , pottery workshop	50 BC –10 AD	P1, D2/4
FEU Can Feu	S. Quirze Vallès (Western Vallès)	<i>Villa</i> , wine centre and pottery workshop	20 BC – 50 AD	P1, D2/4
SAL La Salut	Sabadell (Western Vallès)	<i>Villa</i> , wine centre and pottery workshop	50 BC –10 AD	D1, T1
PRIN Princesa	Barcelona (Barcelonès)	Suburban pottery workshop	20 BC – 1 st c. AD	P1
CPX Can Peixau	Badalona (Barcelonès)	Suburban pottery workshop	40 BC –20 AD	P1
BIF Pompeu Fabra	Badalona (Barcelonès)	Suburban pottery workshop	40 BC – 50 AD	P1, D2/4
CRC Cal Ros Cabres	El Masnou (Maresme)	<i>Villa</i> , wine centre and pottery workshop	30 BC – 1 st c. AD	P1
ACM CAN Pau Ferrer	Cabrera de Mar (Maresme)	Amphorae accumulation	100 – 75 BC	D1
ACM Ca l'Arnau	Cabrera de Mar (Maresme)	Industrial complex, pottery workshop	100 BC –30 AD	D1, T1, P1
MOR El Moré	S. Pol de Mar (Maresme)	Industrial complex, wine centre and pottery workshop	30 BC –20 AD	P1, D2/4
MUJ El Mujal	Ca l'Arnau (Maresme)	<i>Villa</i> , wine centre and pottery workshop	30 BC – 70 AD	T1, P1
FEN Fenals	Lloret de Mar (La Selva)	<i>Fundus</i> , pottery workshop	30 BC –80 AD	P1, D2/4
CAL Collet S. Antoni	Calonge (Baix Empordà)	<i>Fundus</i> , pottery workshop	30 BC –70 AD	P1
LLA Llafranc	Palafrugell (Baix Empordà)	Industrial complex, wine centre and pottery workshop	30 BC – 1 st c. AD	P1, D7/11
PV4 Port- Vendres 4	Port-Vendres (Pyrénées-Orientales)	Shipwreck	40 – 30 BC	P1 and Italian D1 and L2
ULL Els Ullastres	Palafrugell (Baix Empordà)	Shipwreck	25 – 1 BC	P1
CPV Cap del Vol	Port de la Selva (Alt Empordà)	Shipwreck	10 BC – 5 AD	P1

Table 1. The pottery workshops and shipwrecks investigated.

184 Shortly after, around 40-30 BC, a new amphora design, the Pascual 1 (P1) type was
185 adopted in the Laietan region, in the outskirts of the Roman city of *Baetulo* (nowadays
186 Badalona) (CPX, BIF) and at the lower Llobregat River Valley (SBL). Production of P1
187 amphorae spread further throughout the territory, which mirrored the peak of wine
188 industry and trade during Augustus' reign. From that time, it was produced in the
189 pottery workshops that emerged in newly organized territories and cities, such as

190 *Barcino* (Barcelona) (PRI), *Aqua Calidae* (Caldes de Montbui), the western pre-littoral
 191 (FEU), or in the north-eastern (LLA, CAL, FEN, MUJ, MOR) and southern (AUM, ELV)
 192 areas.

193 From 30-20 BC most of the production areas in *Hispania Tarraconensis* started to
 194 imitate another Italian prototype for the wine trade, the Dressel 2/4 (D2/4). The
 195 manufacture of other minor types such as the Oberaden 74 (Ob74) and Dressel 7/11
 196 (D7/11) designs began at this time, the production of which was limited to the northern
 197 and southern areas (Martínez Ferreras, 2014; Miró, 1988).

198 D1, T1, and P1 types were mainly directed for supplying local and Gaul markets,
 199 although the latter also reached military camps in Germania and the southern coasts of
 200 Britannia. Even if some D2/4 were traded to Gaul, this type appears to have been
 201 mainly diffused at a local and regional level or sent to Italy and other areas of the
 202 Roman Empire.

203 The three shipwrecks selected show the trade *in transit* between a port of departure in
 204 NE Spain and a port of destination in southern France, probably at Narbonne (Figure
 205 1). The Port Vendres 4 is one of the several shipwrecks recovered at Port Vendres,
 206 south France. Dated to 40-30 BC, it contained an assemblage of Roman wine
 207 amphorae from Italy (D1 and L2) and NE Spain (P1), suggesting a trade shipment from
 208 a port in the central Catalan coast, probably *Iluro* or *Baetulo*, (Martínez Ferreras et al.
 209 2015). Contrary, Els Ullastres (Palafrugell) and Cap del Vol (Port de la Selva), located
 210 in the northern Catalan coast, comprise homogeneous cargoes including only P1
 211 amphorae. Most of the containers have been associated with the pottery workshops
 212 located on the outskirts of *Baetulo* and particularly, with BIF (Table 2). Therefore, these
 213 two case studies are evidence of the prevalence of the wine amphorae produced at
 214 *Baetulo* (Badalona) in the maritime trade to Gaul during the Augustan Age.

215 2.2. Data formatting

216 We design a database to enclose and relate common aspects of the study of
 217 archaeological pottery from an archaeometric perspective, namely the geochemical,
 218 mineralogical, and petrographic compositions, the latter two being registered as
 219 qualitative data. However, other important attributes relevant to archaeological
 220 interpretations, such as the shape, surface treatment, and mechanical properties could
 221 be introduced, if data is available.

222 The chemical analysis by WD-XRF, the mineralogical analysis by XRD, and the
 223 petrographic analysis through thin section optical microscopy allowed the identification
 224 of specific chemical reference groups (RGs) along the period of activity of the
 225 workshops (Table 2; Martínez Ferreras, 2014).

SITES	RG	AMPHORAE TYPES/SAMPLES*	CaO %	MgO %
AUM (n=10)	AUM-1	P1: AUM-4, 8, 11, 12; D7/11: AUM-14; Ob.74: AUM-17, 20	4.9	5.5
	AUM-2	P1: AUM-5, 10	12.3	4.3
	AUM-IND	P1: AUM-9	5.6	4.3
ELV (n=18)	ELV-1	D1: ELV-2; T3: ELV-7, 9, 15, 52	15.4	3.2
	ELV-2	T3: ELV-45; T1: ELV-51; Flat base: ELV-47, 49	15.7	3.5
	ELV-3	D1: ELV-1; P1: ELV-16, 19, 20, 23, 24, 26, 36	10.7	3.4
	ELV-IND	T3: ELV-28	23.5	2.9

SBL (n=11)	SBL-1	P1: SBL-1, 6, 11, 24, 28, 32	9.2	1.8
	SBL-2	D2/4: SBL-38 e.s. CALAM, SBL-40 e.s. QVA, SBL-42 e.s. QVA, SBL-43 e.s. SAB, SBL-45 e.s. TH	13.3	1.6
FEU (n=20)	FEU-1A	D2/4: FEU-28, 29	4.9	1.8
	FEU-1B	P1: FEU-15, 17, 18, 19, 26	4.9	1.8
	FEU-2A	P1: FEU-1, 3, 5, 6, 8, 13, 14	14.6	1.8
	FEU-2B	Pointed bases: FEU-38 e.s. CE, FEU-39 e.s. CE, FEU-40 e.s. SEVE, FEU-41 e.s. H	12.5	1.7
	FEU-IND1	P1: FEU-9	1.7	2.3
	FEU-IND2	P1: FEU-16	4.9	1.7
SAL (n=11)	SAL-1	D1: SAL-21; T1: SAL-11, 16; Pointed bases: SAL-25 e.s. MAA, SAL-28 e.s. H	6.4	1.5
	SAL-2	D1: SAL-22; T1: SAL-32	8.2	2.1
	SAL-IND1	Pointed bases: SAL-24 e.s. CA, SAL-26 SAL-27 SAL-29	12.6	2.8
	SAL-IND2		2.3	1.9
	SAL-IND3		10.6	1.8
	SAL-IND4		7	3.7
PRINC (n=10)	PRINC-1	P1: CSC-54, 55, 58, 59, 65, 66, 67, 70, 91	7.8	1.9
	PRINC-IND	P1: CSC-85	4.8	2.6
CPX (n=11)	CP-A	P1: CPX-4, 8, 33, MRCCP1 e.s. M.PORCI	12.6	6
	CP-B	P1: CPX-10, 13, 18, 42, 48, MRCCP2 e.s. C.ANTESTI	10.3	4
	CP-IND	T1: MRCCP5 e.s. Q.MEVI	12	3.5
BIF (n=21)	BIF-1	P1: BIF-12, 13, 15, 20	11	8.1
	BIF-2	P1: BIF-4, 5, 6, 9, 11, 21, 25, 28	12.3	5.6
	BIF-3	P1: BIF-19, 41, 48; D2/4: BIF-36, 37	14	7.2
	BIF-IND1	P1: BIF-26	6.3	3.6
	BIF-IND2	D2/4: BIF-35	2.9	1.7
	BIF-IND3	BIF-50	17.3	8.4
CRC (n=5)	CRC-1	P1: CRC-2, 19	14.5	6.8
	CRC-2	P1: CRC-8, 18, 24	13.6	4.3
ACM (n=18)	ACM-A	D1: ACM-73, 80, 86, 97, 99 Can Pau Ferrer	5.2	1.9
	ACM-B	D1: ACM-40, 45, T1D: ACM-59, T1E: ACM-3, 61, 63, P1?: ACM-31 Ca l'Arnau	5.4	1.5
	ACM-C	P1: ACM-1, 20, 71, 72 Ca l'Arnau	11.2	1.6
	ACM-IND1	D1: ACM-81 Can Pau Ferrer	7.9	2
	ACM-IND2	ACM-102 Can Pau Ferrer	5.6	1.6
MOR (n=11)	MOR-1	P1: MOR-4, 5, 6, 10	7.8	1.8
	MOR-2	P1: MOR-8, 13, 15; D2/4: MOR-17	4.4	1.8
	MOR-3	D2/4: MOR-11, 18, Pointed base: MOR-20 e.s. CHR	1.8	1.6
MUJ (n=7)	MUJ-1	P1: MUJ-24, 29	1.2	1.4
	MUJ-2	T1A: MUJ- 40, 41, 42, T1C: MUJ-33, 53	1.4	1.3
FEN (n=9)	FEN-A	P1: FEN-11, 25, 26, 27, 29, 31	1.8	1
	FEN-B	D2/4: FEN-36, 37, 38	1	1.3
CAL (n=6)	CAL-A	P1: CAL-2, 3, 25, 28, 32	13.8	1.6
	CAL-B	P1: CAL-5	5.2	1.6
LLA (n=8)	LLA-A1	P1: LLA-9, D7/11: LLA-13	10	1.3
	LLA-A2	P1: LLA-16, 18, 24, 33, D7/11: LLA-10	5.5	1.3
	LLA-IND	P1: LLA-17	11.9	1.7
PV4 (n=13)	PV4-ACM	P1: PV4-1, 2, 4, 11, 16 e.s. TH+S	3.2	2.5
	PV4-MOR	P1 pointed base: PV4-38 e.s. CHR	1.5	1.5
	PV4-MUJ	P1 pointed base: PV4-8 e.s. AM	1.5	1.4
	PV4-BIF	P1: PV4-5, 7, 9	11.7	6.5
	PV4-IND1	P1: PV4-6	6.9	8.2
	PV4-IND2	P1: PV4-13	11.5	3
	PV4-IND3	P1: PV4-14	12.1	2.2

CDV (n=19)	CDV-BIF	P1: CDV-1-11, 13-15, 17-20	11.4	6.6
	CDV-IND	P1: CDV-12	12.6	8.1
ULL (n=19)	ULL-BIF	P1: ULL-1-4, 7, 9-11, 13-16, 18-20, 22	9	8.8
	ULL-IND1	P1: ULL-12	3.2	2.4
	ULL-IND2	P1: ULL-17	8.6	2.2
	ULL-IND3	P1: ULL-21	2.5	1.7

*e.s.: epigraphic stamp

Table 2. The amphorae examined with indication of the pottery workshops, the groups or productions identified at each one and the average found for CaO and MgO at each group.

226 The geochemical composition was investigated through WD-XRF using a Philips PW
 227 2400 spectrometer with an Rh excitation source. A total of 25 oxides and trace
 228 elements was measured, out of which 16—Fe₂O₃, Al₂O₃, TiO₂, MgO, CaO, SiO₂, Th,
 229 Nb, Zr, Y, Ce, Ga, V, Zn, Ni, and Cr—were deemed fit for the analysis of all samples.

230 The mineralogical composition was examined through XRD using both a Siemens D-
 231 500 and a Panalytical X'Pert PRO alpha 1 diffractometers. The crystalline phases were
 232 evaluated using the PANalytical HighScore X'Pert software and synthesized as an
 233 ordinal variable expressing the approximate firing temperature. Both WD-XRF and
 234 XRD measurements were performed at the CCiT-UB laboratory of the University of
 235 Barcelona.

236 The petrographic measurements were performed through the observation of thin-
 237 sections under the polarising optical microscope Olympus BX41, using a digital camera
 238 Olympus DP70 and the Analysis Five software. Petrographic data concerns the
 239 composition and characteristics of the matrix (groundmass) and the microstructure
 240 (micromass), especially the frequency, size, shape, type, and distribution of non-plastic
 241 inclusions (Whitbread, 1995). The frequency of non-plastic inclusions and voids were
 242 estimated by using the comparative tables offered by Matthew et al. (1991).
 243 Petrographic analysis registered a total of 115 variables, out of which 43 were not
 244 considered in the control study, due to their dependence on known post-depositional
 245 perturbations (Buxeda i Garrigós, 1999; Maritan et al., 2009; Maritan and Mazzoli,
 246 2004; Schwedt et al., 2006) or the absence of variance within the selected samples.

247 In previous studies, we defined fabric groups (FGs), which are broader than RGs,
 248 based solely on petrographic data. Provenance groups (PGs), collapse RGs and FGs
 249 into a wider spatial criterion: e.g., “AUM” means “was made in L’Aumedina’s
 250 workshop”. In all classifications, we tag the site-wise outliers (IND) separately from the
 251 general site groups.

252 A complete list of petrographic variables names and their values can be consulted in
 253 Appendix A.

254 **2.3. Statistical protocols**

255 We defined four protocols using multivariate methods developed and used by
 256 mathematicians, geologists, and ecologists (Anderson and Walsh, 2013; Filzmoser et
 257 al., 2009; Pavoine et al., 2009; Podani, 1999).

258 Protocol 1 is designed for analysing geochemical compositions (CHEM) while protocol
 259 2 aims to represent mineralogical and petrographic data (PETRO). Protocol 3 allows

260 the combination of both types of data (CHEM & PETRO) and can be properly called a
 261 mixed-mode analysis, after Baxter et al. (2008). Protocol 4 is equivalent to protocol 3
 262 but using a specific selection of variables deemed relevant for identifying provenance
 263 (CHEM & PETRO_{PROV}), mainly those indicating mineralogical composition. In addition
 264 to their data source, protocols vary in three key steps: data transformation, calculation
 265 of distance/dissimilarity, and ordination method (Table 3).

Protocol	Protocol 1	Protocol 2	Protocol 3	Protocol 4
Data source	CHEM	PETRO	CHEM & PETRO	CHEM & PETRO _{PROV}
Transformation	ilr/clr	ranking	clr & ranking	clr & ranking
Distance	Euclidean	RRD/NI	Extended Gower distance (Euclidean & RRD)	Extended Gower distance (Euclidean & RRD)
Ordination	RPCA	PCoA/NMDS	PCoA	PCoA

Table 3. Statistical protocols

266 Focusing in CHEM, the protocol 1 first step is to transform counts or percentages given
 267 by WD-XRF readings into log-ratios (Aitchison, 1982; Buxeda i Garrigós, 1999; Martín-
 268 Fernández et al., 2015; Pawlowsky-Glahn and Buccianti, 2011). Once data is
 269 transformed using any log-ratio procedure (alr, clr, or ilr), it is possible to perform PCA
 270 using Euclidean distances between log-ratios. However, we do warn that using
 271 different log-ratio transformations, as well as any other transformation (normalization,
 272 logarithmic), must be taken into account carefully while interpreting results. For
 273 easiness and readability, we followed the approach of Filzmoser et al. (2009), which
 274 uses a combination of ilr transformation and RPCA. Such treatment empowers the
 275 visualisation of compositional data, by compensating for distortions produced by
 276 outliers and closure. There are three R packages dedicated to compositional data
 277 (zCompositions: Palarea-Albaladejo and Martín-Fernández, 2015; robCompositions:
 278 Templ et al., 2011; compositions: van den Boogaart et al., 2014).

279 When addressing PETRO in protocols 2, 3, and 4, we chose to preserve the original
 280 format of variables—i.e., ordinal variables. This practice contrasts with other
 281 approaches (Baxter et al., 2008; Cau Ontiveros et al., 2004; Ownby et al., 2014).
 282 These used binominal dummy variables instead, thus merely differentiating values
 283 (e.g., “common” ≠ “few”) instead of accounting for their order (e.g., “common” > “few”).
 284 However, a special treatment is required to measure dissimilarity in ordinal variables.
 285 We explored two alternative approaches to this challenge, relative rank difference and
 286 neighbour interchange (NI and RRD; Appendix B; Podani, 1999). The essential trait of
 287 both methods is that ordinal values are converted into rank scores, which depend not
 288 only on ordering (i.e., the sequence of categories) but also on ties (i.e., observations
 289 falling into the same category).

290 Dissimilarities given by NI generally do not satisfy the axiom of triangle inequality (i.e.,
 291 they are not metric). Therefore, NI can be used in protocol 2, dealing only with ordinal
 292 variables, but it is incompatible with the integration of Euclidean distances, as in
 293 protocols 3 and 4. In turn, RRD dissimilarities can be analysed with metric techniques
 294 and so we used this approach to measure dissimilarity in PETRO variables in protocols
 295 2 through 4.

296 Protocols 2 through 4 calculate the overall dissimilarity between observations using a
297 version of Gower's distance (Gower, 1971; Appendix B), extended and implemented in
298 R language by Pavoine et al. (2009). Similarly to Baxter et al. (2008) 'mixed mode'
299 approach, they named this methodology as the "mixed-variables coefficient of distance"
300 which was presented with their original R code.

301 The extended Gower distance enables protocols 3 and 4 to combine CHEM and
302 PETRO in the same distance coefficient. CHEM numeric variables contribute with
303 Euclidean distances between pairs of clr, and PETRO ordinal variables with RRD
304 between pairs of rank scores. By modifying Pavoine et al. (2009) original script, it was
305 possible to equal the weights of the two sets of variables (CHEM, PETRO), so that the
306 distance represents the exact middle ground between the patterns displayed in
307 protocols 1 and 2. We then project the resulting distance matrix in 2D and 3D through
308 PCoA.

309 The 2D and 3D projections generated by each protocol are complemented with
310 PERMANOVA and PERMDISP2 tests (Anderson and Walsh, 2013), which together
311 evaluate the significance of the separation between given groups. These tests are
312 good supplements to ordination methods (PCA, PCoA) because both use the entire
313 multidimensional variability present in distance matrices, part of which is invisible in
314 graphic projections (biplots).

315 PERMANOVA assesses the probability of the null hypothesis of no difference among
316 group centroids (i.e., small p values indicate significant separation). However,
317 PERMANOVA is unreliable when there is heterogeneity of dispersions, which
318 confounds effects of group location and dispersion. PERMDISP2 tests the null
319 hypothesis of heterogeneity of dispersions, ignoring the position of group centroids. If
320 homogeneity of dispersion can be assured (PERMDISP2: p-value < 0.05),
321 PERMANOVA may be considered a reliable test for significant separation among
322 groups. Both tests are possible using the *vegan* package in R (Dixon, 2003; Jari
323 Oksanen et al., 2016): the *adonis* function and the *permtest* function (applied to
324 *betadisper* function results).

325 The statistical protocols presented here include methods already available in one or
326 more existing packages in R. However, we aim to facilitate their use for archaeologists.
327 In this sense, accompanying this study, we present two R packages that are fully
328 documented and freely available.

329 The *cerUB* package contains all necessary functions to follow the protocols and apply
330 them to other comparable datasets (Angourakis and Martínez Ferreras, 2017). It
331 includes the dataset presented here (amphorae), as a working example but also for
332 ease of reproducibility.

333 The *biplot2d3d* package (Angourakis, 2017) combines the functionalities of several R
334 packages to generate 2D and 3D projections of ordination methods (biplots; Gabriel,
335 1971), allowing for centralized control of many graphic parameters. We used four
336 features particular to this package:

- 337 1. We opted to detach the location of the 'second' plot of a biplot (i.e., the arrows),
338 move it to the bottom-right corner, and re-scale it to avoid overlapping points;

- 339 2. To reduce the number of variables represented in protocols using petrographic
340 data (>80 variables), we filtered those that did not project well in the first two
341 dimensions (less than 50% of the maximum covariance among all variables).
- 342 3. We added a representation of eigenvalues (bottom-left corner), which are
343 interpretable as the proportion of variance captured in every dimension (i.e., the
344 first two or three bars being the dimensions of the plot). Additionally, we indicate
345 this proportion as the percentage of variance explained by the visible
346 dimensions.
- 347 4. We mark groups with inertia ellipses, which correspond to 95% confidence
348 ellipses whenever we assume that group members were drawn from normal
349 distributions for all input variables. We advise that this may not be reasonable
350 for groups that are either too small or contain subgroups, in which case ellipses
351 should be interpreted simply as graphic summaries of the group's cloud of
352 points. We also add the "star" representation of groups, i.e. every point
353 connected by a line to the centroid.

354 We offer a full walkthrough for installing and using the *cerUB* and *biplot2d3d* packages
355 (Appendix C) and the corresponding R scripts (Appendix D); both are also available in
356 a GitHub page (https://andros-spica.github.io/cerUB_tutorial/). Besides having
357 published them in Zenodo.org, we maintain their open source code in GitHub
358 repositories (github.com/Andros-Spica/cerUB, github.com/Andros-Spica/biplot2d3d). All
359 analyses and plots presented here were made using R 3.4.1.

360 **3. Results**

361 **3.1. Determining production centres**

362 Aiming to test their usefulness for defining productions from pottery centres, we applied
363 protocols 1 through 4 only to samples found in workshops. The classifications
364 displayed in biplots and tested with PERMANOVA and PERMDISP2 vary depending on
365 the range of the input data (i.e., RGs in protocol 1 and 3, FGs in protocol 2, and PGs in
366 protocols 4).

367 In Protocol 1 (Figure 2; Appendix E.1), the amphorae are distributed forming clusters
368 consistent with the previously defined RGs. Most IND sherds are isolated or close to
369 other sites' RGs. The main factors causing this distribution are the CaO and MgO
370 values. As already detected, the P1 produced around *Baetulo* has the highest MgO
371 content (Buxeda i Garrigós et al., 2002; Martínez Ferreras, 2014).

387 A), and D2/4 (FEN-B) types, also joined by one of the pointed bases from La Salut
388 (SAL-IND2). This cluster exhibits the lowest CaO (1-2%) of the dataset, together with
389 low MgO and high Fe₂O₃, Al₂O₃, SiO₂, Zr, and Y. Nevertheless, amphorae from FEN
390 present lower TiO₂ and V, and higher Cr values. Most of the D2/4 from MOR (MOR-3)
391 resemble these productions, although they exhibit lower Cr and higher Zn. The P1 from
392 MOR (MOR-2) are low to border calcareous (4% CaO), while the earlier production of
393 this type (MOR-1) appears to be calcareous (7-8% CaO).

394 In ACM, the production of different types of amphorae also entailed changes in raw
395 materials procurement or processing. For instance, the D1 and T1 (ACM-A and ACM-
396 B) exhibit 4-7% CaO and high Fe₂O₃, Al₂O₃, TiO₂, Y, and Ce. Their composition is
397 similar to MOR-2, though with higher Cr. The P1 and D2/4 from FEU (FEU-1A and
398 FEU-1B) resemble ACM's but containing higher Zn and Ni. We could attribute the P1
399 PRINC-IND found at Barcelona to FEU productions. The D1 and T1 from SAL (SAL-1)
400 are border calcareous (6.4% CaO) with high TiO₂ and Zr. Instead, SAL-2 is more
401 calcareous and exhibits lower Zr and Cr.

402 The P1 from PRINC (PRINC-1) and LLA (LLA-A1) are also border calcareous to
403 calcareous with low Fe₂O₃ and Al₂O₃. LLA-A1 presents lower MnO, TiO₂, and MgO,
404 and higher Cr. It differs from LLA-A2 because the latter exhibits higher CaO (10%). The
405 calcareous P1 LLA-A2 is similar to CAL-A, ACM-C, and SBL-1. Ce is higher in ACM-C,
406 while Ni and Cr are more abundant in SBL-1. The D2/4 from SBL (SBL-2) exhibits
407 lower Zr and Cr, and present similarities with the P1 from FEU (FEU-2A and FEU-2B),
408 except for their higher SiO₂. One of the pointed bases from SAL (SAL-IND-3) also
409 resembles these two FEU RGs.

410 The P1 discussed above differ from those produced at the Besòs River Valley, through
411 their MgO content. Amphorae from CP (CP-A and CP-B) and BIF (BIF-1, BIF-2, and
412 BIF-3) consist of calcareous pastes (10-14% CaO) with low Al₂O₃, SiO₂, and Ga, and
413 high MgO (4-8%). As previously suggested, amphorae from *Baetulo* resemble those
414 found at CRC (CRC-1/2), located north of the Roman city (Buxeda i Garrigós et al.,
415 2002).

416 Regarding the southern workshops near *Tarraco* (Tarragona), some RGs present a
417 relatively unique chemical composition, i.e., the D1, T3, and flat-bottom amphorae from
418 ELV-1 and ELV-2 and the P1 from AUM-1. The first two present calcareous pastes (15-
419 16% CaO) with high Ni and low Al₂O₃, SiO₂, Ce, and Ga, while the third exhibits 5%
420 CaO, the highest K₂O (5%), high MgO (5.5%) and Ni, and low SiO₂, Ba, Zr, and Ce.
421 Nevertheless, the P1 from ELV-3 contain higher Ce and Zn and are closer to the P1
422 from CP-B. Moreover, the two amphorae included in group AUM-2 exhibit higher CaO
423 (12%), Sr, and Cu and approach the products from *Baetulo*.

424 We mentioned the interesting cases of those IND sherds found in one workshop but
425 allegedly produced in another. However, most INDs (AUM-IND1, FEU-IND2, BIF-IND1,
426 BIF-IND3, ACM-IND1, and ACM-IND2) are linked with the RGs of their respective sites.
427 They probably correspond to productions that were not well characterised, or were
428 made in nearby workshops not yet investigated or discovered. Only two samples, FEU-
429 IND1 and ELV-IND1, don't match with any RG and so their provenance remains
430 indeterminate.

431 In protocol 2, the separation of FGs is more consistent with their textural characteristics
 432 and with the geographical location of the pottery workshops (Figure 3; Appendix E.2).
 433 For instance, the amphorae from the southern workshops (AUM and ELV) are tightly
 434 clustered because they consist of fine to medium-fine fabrics with moderately abundant
 435 aplastic inclusions (≤ 0.5 mm grain-sized; lower L2; Figure 4). The predominant
 436 inclusions are quartz (L43), K-feldspar, and plagioclase derived from granitoids.
 437 Foraminifers, micritic calcite (L27), and sparite in some samples, all presenting various
 438 states of decomposition, are frequent. Phyllosilicates (L36), metamorphic and
 439 sedimentary rock fragments (L24, L33) are common to few. The raw materials used
 440 were the local Pleistocene alluvial deposits and piedmont terrains constituted by marls,
 441 calcarenites, and biomicrites from the Miocene.

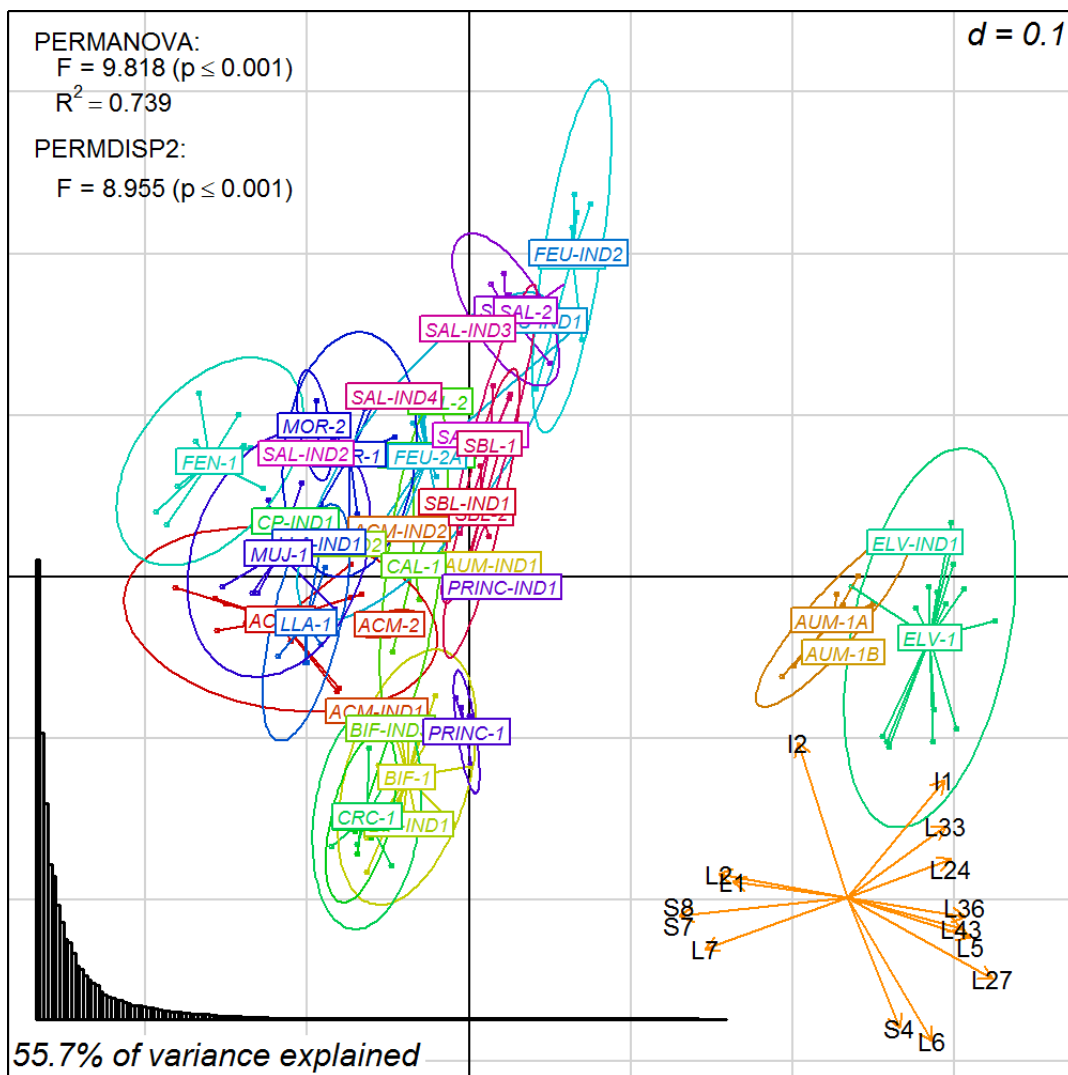


Figure 3. Protocol 2 results concerning workshops samples. The plot shows the best 2D projection, the horizontal and vertical axes respectively containing the first and second principal coordinates. The FGs are labelled and distinguished by colour. Consult Appendix A for variable codes.

442 The coarser, low calcareous D1, T1, and P1 from the workshops located around *Iluro*
 443 and *Blandae* —ACM-1 MOR-1 and MOR-2, MUJ-1, and FEN-1— appear on the
 444 opposite side. These workshops exploited raw materials from the Quaternary fluvial-
 445 torrential deposits extending in the narrow plain between the coastal mountains and the

446 Mediterranean Sea. The clayey matrix is rich in iron oxides, and inclusions are
447 moderately abundant, ranging in size from fine-grained to very coarse-grained sand (\leq
448 0.25-2 mm grain-sized; higher L2). They include predominant granitic rock fragments
449 (L7) derived from the Carboniferous-Permian coastal mountain system and crystals
450 detached from these rocks, mainly quartz, K-feldspar, plagioclase, and biotite together
451 with few to common amphibole and epidote (Figure 4). Partly or totally decomposed
452 microfossils and calcite (micrite) are common to rare in fabrics ACM-1, MOR-1 and
453 LLA-1. MOR-1 and MOR-2 exhibit few metamorphic rock fragments. Moreover,
454 clinopyroxene crystals are present (few) in LLA-1 derived from the Quaternary alkaline-
455 volcanic complex located to the west. Although overlapping in 2D, ACM-1 and LLA-1
456 are well differentiated in 3D.

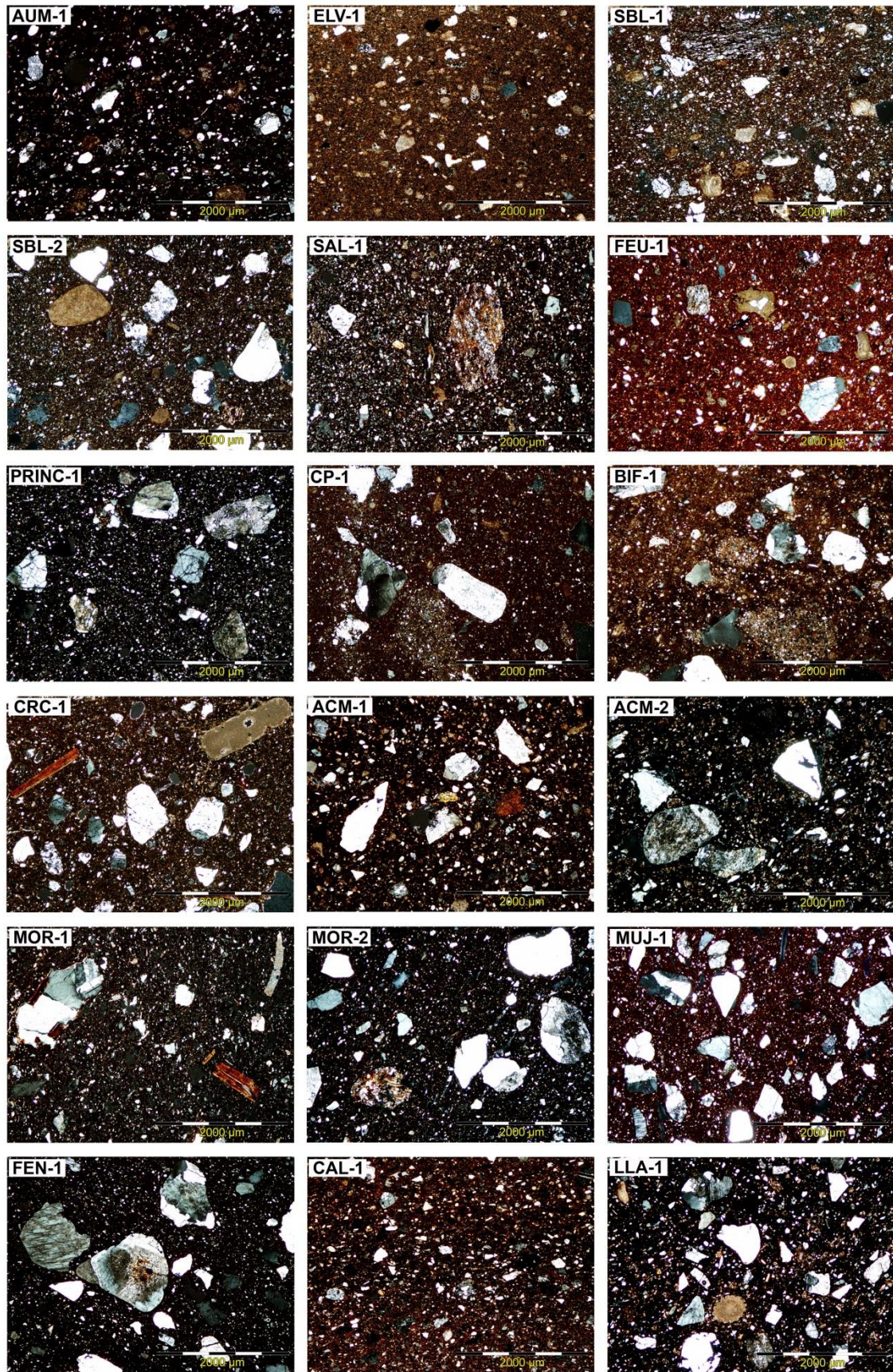


Figure 4. Microphotographs of the FGs 40X, XPL

457 A few P1 from CAL (CAL-2) are close to those of *Iluro* and *Blandae* because it
458 corresponds to a medium coarse, border calcareous fabric with few microfossils and
459 frequent crystals derived of granitoids. The other P1 from this workshop (CAL-1) are
460 not too different, though they have a Ca-rich matrix with predominant inclusions of
461 grain size fine to medium-fine (Vila Socias and Martínez Ferreras, 2015). Despite its
462 finer inclusions, the petrographic composition of CAL amphorae resembles that of the
463 P1 from ACM (ACM-2).

464 The fabrics attributed to the sites near the Ripoll River Basin (FEU-1, SAL-1, and SAL-
465 2), as well as some “IND” sherds from these sites, are clustered because they consist
466 in medium-to-coarse, border calcareous to calcareous fabrics. The clayey sediment is
467 rich in iron oxides, with the presence of some nodules of calcite (micrite) and
468 microfossils, especially in SAL-2. Most of the inclusions are metamorphic and
469 sedimentary rock fragments, together with crystals derived from granitoids. They
470 constitute the fluvial-torrential Miocene and Quaternary clayey sediments of the Ripoll
471 River Valley formed by the erosion of the littoral and pre-littoral mountain ranges.

472 FEU-2 and the productions from the Lower Llobregat basin (SBL-1 and SBL-2) and
473 Barcelona (PRINC-1) unite because they all are calcareous, coarse fabrics. FEU-2
474 comprises P1 and pointed bases with epigraphic stamps that were produced using Ca-
475 rich clays with abundant medium to very coarse grain-sized aplastic inclusions. In this
476 case, granitic and metamorphic rock fragments predominate, quartz and feldspars are
477 frequent, and limestone and fragments of sedimentary rocks are scarce. The P1 from
478 SBL-1, SBL-2, and PRINC-1 have in turn a Fe-rich clay matrix with carbonates and
479 moderately abundant inclusions, which primarily consist of granitic rock fragments,
480 crystals derived from these rocks, metamorphic rock fragments and, to a lesser extent,
481 sedimentary rock grains. These materials come from the Quaternary alluvial clayey
482 sediments deposited in the Lower Valley of the Llobregat River.

483 The coarse FGs from CP and BIF, in *Baetulo* (CP-1 and BIF-1), and CRC (CRC-1) are
484 clustered apart because they exhibit a characteristic calcareous matrix with aggregates
485 of calcareous, silty sediment. The aplastic inclusions are relatively abundant and
486 consist of coarse and very coarse granitic rock fragments and crystals derived from
487 these rocks —quartz, plagioclase, K-feldspar, amphibole, and epidote— along with
488 calcareous nodules (micrite). Sandstone and metamorphic rock fragments are few or
489 absent at CP-1.

490 Protocol 3 represents an amalgam of the technological characteristics of productions
491 and their provenance, by combining all CHEM and PETRO variables (Figure 5,
492 Appendix E.3).

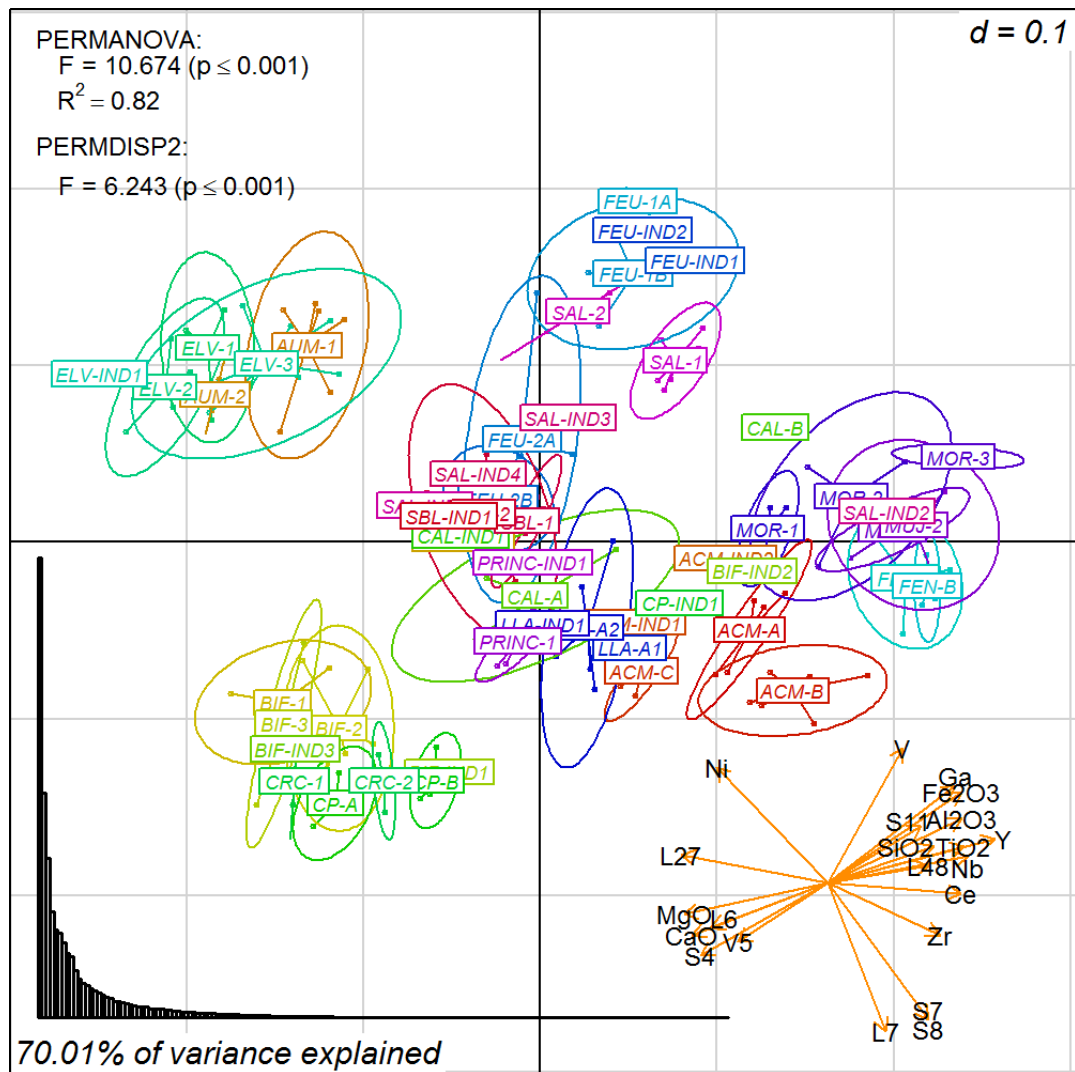


Figure 5. Protocol 3 results concerning the workshops samples. The plot shows the best 2D projection, the horizontal and vertical axes respectively containing the first and second principal coordinates. The RGs and the site outliers are labelled and distinguished by colour. Consult Appendix A for variable codes.

493 The southern workshops (AUM and ELV) stand out from the others. The most
 494 distinctive characteristic is their fine fabrics, predominantly calcareous, with an
 495 abundance of carbonates, especially foraminifers, quartz, feldspars, and metamorphic
 496 and sedimentary rock fragments.

497 Workshops near *Iluro* and *Blandae* (ACM, MOR, MUJ, and FEN) differ because of their
 498 Fe-rich clays with coarse aplastic inclusions primarily derived from granitoids and
 499 abundant biotite, consistent with high Fe_2O_3 , Al_2O_3 , and SiO_2 . The amphorae from the
 500 Lower Besòs Basin (CP, BIF and CRC), already well distinguished with protocols 1 and
 501 2, are completely detached from the other workshops. In protocol 3, their position is
 502 due to both their petrographic properties (coarse fabrics with a predominance of
 503 carbonates and crystals and rock fragments derived from granitoids in a Ca-rich clay
 504 matrix) and their high CaO and MgO contents, which are consistent with the presence
 505 of dolomite outcrops in the area.

506 FEU and SAL form another cluster. The D1 and T1 from SAL are close to the border
 507 calcareous P1 and D2/4 from FEU (FEU-1A and FEU-1B). Less distinguished, the
 508 calcareous P1 and pointed bases with stamped marks from FEU (FEU-2A and FEU-
 509 2B) share significant compositional similarities with the D2/4 from SBL (SBL-2). They
 510 consist of calcareous, coarse amphorae, with granitoids, metamorphic and sedimentary
 511 rock fragments and carbonates resulting in high CaO and low Fe₂O₃, Al₂O₃, MgO, and
 512 Cr. The P1 from SBL (SBL-1) differ from SBL-2 because they contain higher Zr, Ni, and
 513 Cr. They chemically resemble the P1 of PRINC-1, but the lithological constituents of
 514 the aplastic inclusions are equivalent to those observed in the D2/4 from SBL-2.

515 The northern workshops (CAL and LLA) are difficult to individualize. The calcareous P1
 516 (CAL-A and LLA-A2), which contain foraminifers and bivalves, match those of SBL-1
 517 and PRINC-1. On the other hand, the border calcareous P1 and D7/11 of LLA-A1 are
 518 closer to the calcareous P1 of ACM-C.

519

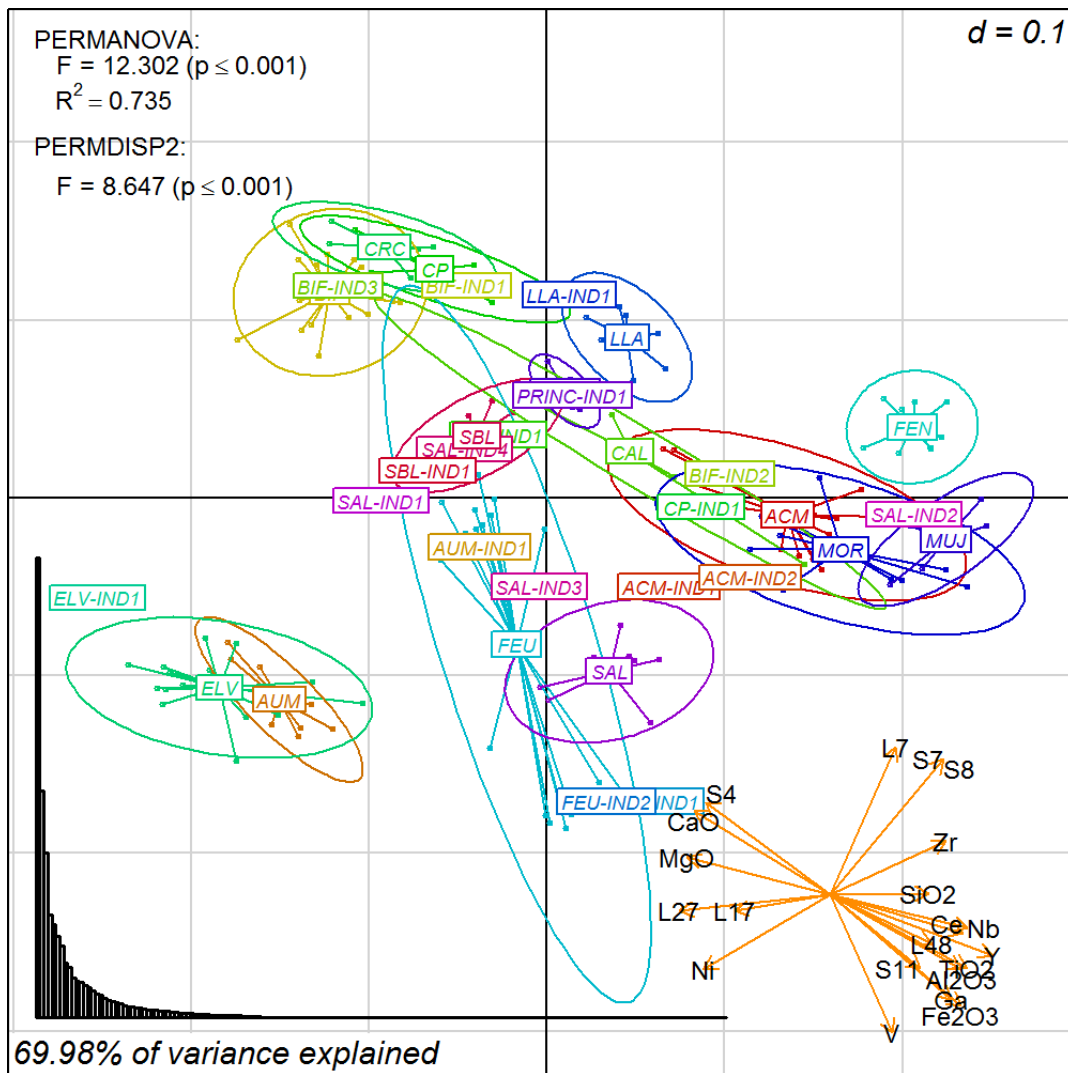


Figure 6. Protocol 4 results concerning the workshops. The plot shows the best 2D projection, the horizontal and vertical axes respectively containing the first and second principal coordinates. The general PGs and the site outliers are labelled and distinguished by colour. Consult Appendix A for variable codes.

520 To assess the provenance as accurately as possible, protocol 4 considers only
521 variables that characterize raw materials (CHEM & PETRO_{PROV}). The resulting biplot
522 (Figure 6; Appendix E.4) were not as discriminative as expected. This is due to the still
523 high multidimensionality of the data—note the many long arrows pointing different
524 directions. Even so, several productions are individualised and most positions are
525 consistent with the PGs.

526 Particularly well defined are the workshops placed near the Ebro River and *Tarraco*
527 (AUM and ELV), in the lower Besòs River Basin near *Baetulo* (CP, BIF, CRC), and in
528 the Laietan region near *Iluro* and *Blandae* (ACM, MOR, MUJ, FEN). CP, BIF, and CRC
529 exploited Holocene deposits and Miocene marls from the plain that are deltaic, fluvial,
530 torrential and marine. The presence of carbonates in the clayey pastes conferred pale
531 brown to yellowish colours after firing. Instead, the amphorae produced in ACM, MOR,
532 MUJ, and FEN consist in reddish fabrics because the Laietan potters employed the Fe-
533 rich clayey sediments from Quaternary fluvial-torrential deposits that cover the littoral
534 plain. These areas have specific geological constituents, and their amphorae
535 productions are well differentiated while the variability within each zone is very low.

536 Unfortunately, not even protocol 4 can satisfactorily separate all productions within
537 each region. Nonetheless, this treatment proved to be useful to discern among the
538 amphorae manufactured in the Ripoll River Basin (FEU and SAL), even when they
539 exhibit a high variability in shapes and composition within their workshops. It also
540 allowed individualizing LLA, PRINC, and SBL, which overlap in other protocols. CAL
541 remains the only workshop that overlaps in 2D with geographically unrelated
542 productions.

543 **3.2 Determining provenance: Shipwreck case studies**

544 Protocol 4 proved to be the most effective treatment for individualizing provenance.
545 Therefore, we used it to explore the origin of amphorae from the three shipwrecks
546 considered in this study.

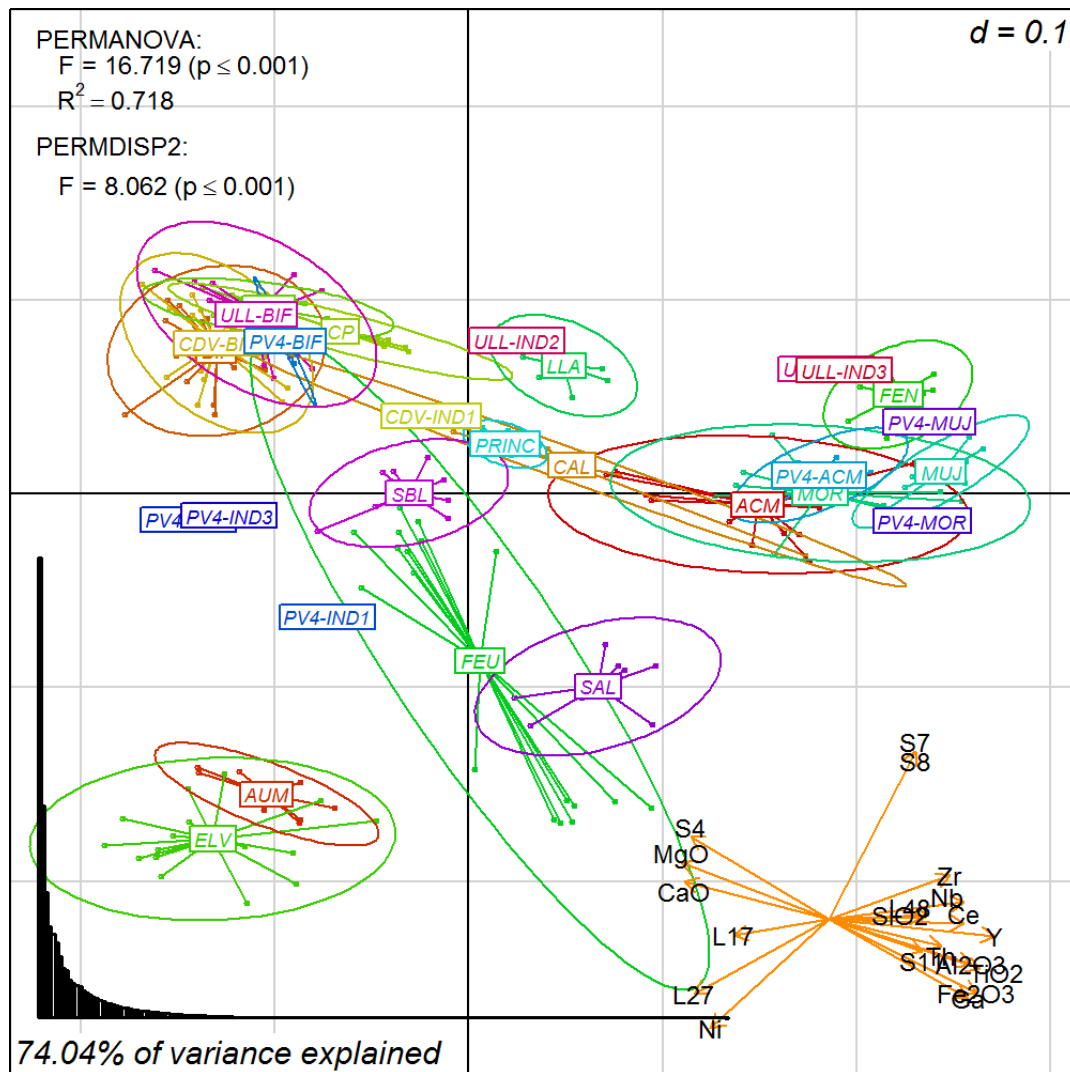


Figure 7. Protocol 4 results concerning both workshops and shipwrecks samples. The plot shows the best 2D projection, the horizontal and vertical axes respectively containing the first and second principal components. The general PGs and the shipwreck outliers are labelled and distinguished by colour. Consult Appendix A for variable codes.

547 As expected, the biplot (Figure 7; Appendix E.5) shows that most of the P1 from CDV
 548 (CDV-BIF) and ULL (ULL-BIF), dated to the Augustan Age, match the amphorae
 549 produced at the lower Besòs River Basin (CP, BIF and CRC). Two of the containers
 550 with unknown origin from ULL (ULL-IND1/3) resemble the low calcareous productions
 551 from MUJ and FEN, while ULL-IND2 is closer to the productions of LLA. CDV-IND1
 552 appears related to the amphorae produced at the lower Llobregat River Valley (SBL)
 553 and *Barcino* (PRINC). Despite the varied provenance of these amphorae, the port of
 554 departure of these ships was probably the coastal city of *Baetulo* since most of the
 555 cargo originated in either one of the two workshops found on the outskirts of the city
 556 (BIF, CP).

557 Dated in earlier times (between 40-30 BC), the provenance of the amphorae found in
 558 PV4 is more diverse. Some low and border calcareous amphorae (PV4-ACM, PV4-
 559 MOR, and PV4-MUJ) present similar chemical and petrographic composition with the
 560 products of different workshops located in the territory of *Iluro* and *Blandae* (i.e., ACM,
 561 MOR, and MUJ). Other vessels are associated with the workshops in *Baetulo* (PV4-

562 BIF), and three (PV4-IND1/2/3) are isolated due to major chemical and petrographic
563 differences compared to the PGs considered.

564 **4. Discussion**

565 The goal of this paper has been to present an explorative methodology for analysing
566 the variability of archaeological ceramics. We intended to offer alternative protocols
567 that drawn information from different data sources and follow different statistical
568 treatments. Building on the conclusions of Baxter et al. (2008), we experimented with a
569 new version of what they named the mixed-mode approach, i.e., the combination of
570 geochemical composition and petrographic data into the same multivariate analysis.
571 Their proposal included using raw chemical data and converting petrographic ordinal
572 data into binominal dummy variables, and the application of PCA or CA for
573 visualization. The approach we advocate here differs in that geochemical data is
574 treated as compositional data, by applying log-ratio transformations, and that the
575 ordinal variables normally used as petrographic data can contribute to more systematic
576 analysis without sacrificing the ordering information. In this sense, our proposal
577 employs techniques developed in other disciplines that, in our assessment, produce
578 more satisfactory and integral images of ceramic materials.

579 Our confidence in the protocols presented here comes from their performance
580 summarizing the variability of the Roman wine amphorae as shown above. Overall,
581 there is a good match between prior classifications (RGs, FGs, and PGs) and the
582 2D/3D projections generated by each protocol. Additionally, all PERMANOVA and
583 PERMDISP2 results are significant, under any reasonable criterion (in all cases p-
584 values are much less than 0.01), meaning that the classifications given are satisfactory
585 group hypotheses according to the distances calculated in each protocol.

586 Except in protocol 1 where there is much overlap, 2D projections consistently
587 separated the two southern workshops (ELV, AUM), the three *Baetulo*-Besòs river
588 workshops (BIF, CP, CRC), four of the Laietan workshops (ACM, MOR, MUJ, FEN),
589 and, in lesser degree, the two inland workshops (SAL, FEU). The least differentiated
590 groups were those containing samples from SBL, PRINC, and CAL, which never lay
591 too far from the projection centre.

592 By comparing the results of the four protocols, we also aimed to present an
593 independent confirmation of the main conclusion in Baxter et al. (2008), which states
594 that the 'mixed mode' approach to archaeological ceramics is superior to considering
595 data sources separately. Indeed, the results obtained with protocols 3 and 4 confirmed
596 that integrating *chemical* and *petrographic* data can aid characterization and the
597 detection of groups in space and time. Furthermore, we concluded that a more
598 selective multivariate analysis is a better strategy for answering specific questions—
599 i.e., choosing those variables known to indicate the provenance of materials in protocol
600 4.

601 To the date, several studies in pottery archaeometry use more than a single analytic
602 method, typically WD-XRF and petrographic observations. In this sense, they are
603 already following a 'mixed mode' approach. However, datasets originating from
604 different sources are rarely put together into the same database or go through the

605 same statistical analysis, if at all. By publishing online the *cerUB* and *biplot2d3d*
606 packages, we offer an opportunity for those researchers that have access to different
607 analytic methods but lack the know-how required for applying and visualizing more
608 sophisticated multivariate statistics (including ordinal variables). Moreover, by
609 establishing these four protocols under the same framework, we allow for
610 straightforward comparisons between their results, which is useful for defining and
611 testing typologies based on different aspects of the data.

612 Despite what, in our opinion, are clear advantages of applying these protocols, we did
613 detect possible caveats in doing so. First, the applicability of protocols 2 through 4
614 requires petrographic observations to be annotated in a database. Due to the amount
615 of work this entails, petrographic variables may not be available for all archaeological
616 samples recovered. However, it is indispensable that observations entering the
617 database take the form of ordinal variables rather than other qualitative textual
618 assessment. Additionally, the functions in *cerUB* package assume that petrographic
619 data were named and entered following the same system used by us (Appendix A).
620 However, as we have shown here, it is not necessary to input all petrographic variables
621 in our list since protocols can manage any smaller set of variables.

622 Also, if the analyst has access to a reliable quantitative petrographic method (e.g.,
623 point-counting), other versions of protocols 2, 3, and 4 could be developed to only
624 handle sets of numeric variables rather than using ordinal variables. In the case of
625 using point counting, these alternative protocols would certainly be less complex,
626 requiring solely the scaling to sample total (in case totals vary among samples) and a
627 log-ratio transformation, given that the input data is strictly compositional (as defined in
628 Aitchison, 1982).

629 Another critical warning concerns the nature of multivariate representations (e.g.,
630 biplots), not only in our protocols but when using any ordination method (e.g., PCA,
631 CA, PCoA). We cannot interpret a multivariate projection as bivariate. Multivariate
632 means multidimensional, which implies that the distance between two points in two
633 dimensions cannot account for their distance in a third dimension, the same way that a
634 single blueprint cannot represent a two-story building. Biplots of the first two principal
635 coordinates display the most complete 2D representation that the method can calculate
636 with the data given.

637 For instance, in protocol 1 (Figure 2), the 2D projection explains almost 80% of the total
638 variability, which in turn is mostly contributed by CaO and MgO. In this case, we may
639 read more safely the position of points in terms of more or less CaO or MgO content.
640 Conversely, when there are many variables, the two most explicative dimensions may
641 correlate with several of them, what is represented in a biplot as a star of long arrows
642 pointing out many directions. In this kind of context, variables 'compete' with each other
643 to order the points according to their criterion. This is the case in protocol 2 (Figure 3),
644 where the orientation of inclusions (I2) has a clear readability while interpreting, for
645 instance, the presence-abundance of chert (L33) can be misleading. The Appendix
646 section C.8 explains this more thoroughly.

647 With this paper we hope to provide general archaeologists with a tool for accessing a
648 straightforward image of the variability of their ceramic materials, thus assisting

649 archaeological classification. However, this is an exploratory tool, and it is not designed
650 to replace finer analyses of geological provenance and material science. Nor do we
651 suggest dismissing other classical multivariate approaches, which are also readily
652 available in R (Baxter, 2016). In this sense, the end products of the protocols (i.e., an R
653 list object) contain a distance matrix that can be further used in other multivariate
654 methods, such as discriminant and cluster analysis. We do not discard the possibility of
655 applying this type of methodology in other archaeological materials and we encourage
656 future development in this direction.

657 **Acknowledgements**

658 We would like to thank Dr J. Buxeda i Garrigós and Dr Ll. Vila Socias for providing us
659 with chemical results from several workshops, as well as Dr. Patrick Quinn for several
660 suggestions concerning the display and evaluation of protocols results. We also are
661 very grateful for the corrections, comments, and suggestions of the anonymous
662 reviewers.

663 Funding: This work was supported by the R&D&I projects CAMOTECCER (HAR2012-
664 32653) and CERAC (HAR2016-75133-C3-1-P) led by V. Martínez and J.M. Gurt, and
665 funded by the Spanish Ministry of Economy and Competitiveness (MINECO). A.
666 Angourakis worked on this paper through the FPI contract (BES-2013-062691), and V.
667 Martínez through the post-doctoral research contract Ramón y Cajal (RYC-2014-
668 15789), all funded by MINECO.

669

670 **References**

671 Aitchison, J., 1982. The Statistical Analysis of Compositional Data. *J. R. Stat. Soc. Ser. B* 44, 139–
672 177.

673 Anderson, M.J., Walsh, D.C.I., 2013. PERMANOVA, ANOSIM, and the Mantel test in the face of
674 heterogeneous dispersions: What null hypothesis are you testing? *Ecol. Monogr.* 83, 557–
675 574. doi:10.1890/12-2010.1

676 Angourakis, A., 2017. biplot2d3d - an R package for generating highly-customizable biplots.
677 Zenodo. doi:10.5281/zenodo.889704

678 Angourakis, A., Martínez Ferreras, V., 2017. cerUB - Protocols for exploring archaeometric data
679 (R package). Zenodo. doi:10.5281/zenodo.975450

680 Baxter, M.J., 2016. *Multivariate Analysis of Archaeometric Data: An Introduction*.
681 Academia.edu.

682 https://www.academia.edu/24456912/Multivariate_Analysis_of_Archaeometric_Data_A

683 n_Introduction.

684 Baxter, M.J., 2008. Mathematics, statistics and archaeometry: The past 50 years or so.
685 Archaeometry 50, 968–982. doi:10.1111/j.1475-4754.2008.00427.x

686 Baxter, M.J., Beardah, C.C., Papageorgiou, I., Cau Ontiveros, M.-Á., Day, P.M., Kilikoglou, V.,
687 2008. On statistical approaches to the study of ceramic artefacts using geochemical and
688 petrographic data. Archaeometry 50, 142–157. doi:10.1111/j.1475-4754.2007.00359.x

689 Buxeda i Garrigós, J., 1999. Alteration and Contamination of Archaeological Ceramics: The
690 Perturbation Problem. J. Archaeol. Sci. 26, 295–313. doi:10.1006/jasc.1998.0390

691 Buxeda i Garrigós, J., Comas i Solà, M., Gurt Esparraguera, J.M., 2002. Roman amphorae
692 production in Baetulo (Badalona, Catalonia). Evidence of Pascual 1, in: Kilikoglou, V.,
693 Hein, A., Maniatis, Y. (Eds.), Modern Trends in Scientific Studies on Ancient Ceramics. BAR
694 International Series 1011, Oxford, pp. 277–285.

695 Cau Ontiveros, M.-Á., Day, P.M., Baxter, M.J., Papageorgiou, I., Iliopoulos, I., Montana, G.,
696 2004. Exploring automatic grouping procedures in ceramic petrology. J. Archaeol. Sci. 31,
697 1325–1338. doi:10.1016/j.jas.2004.03.006

698 Cressell, R., 1990. “A New Technology” Revisited. Archaeol. Rev. from Cambridge 9, 39–54.

699 Dixon, P., 2003. VEGAN, a package of R functions for community ecology. J. Veg. Sci. 14, 927–
700 930. doi:10.1111/j.1654-1103.2003.tb02228.x

701 Filzmoser, P., Hron, K., Reimann, C., 2009. Principal component analysis for compositional data
702 with outliers. Environmetrics 20, 621–632. doi:10.1002/env.966

703 Gabriel, K.R., 1971. The biplot graphic display of matrices with application to principal
704 component analysis. Biometrika 58, 453–467. doi:10.1093/biomet/58.3.453

705 Gandrud, C., 2016. Reproducible research with R and RStudio. Chapman and Hall/CRC Press.

706 Gower, J.C., 1971. A General Coefficient of Similarity and Some of Its Properties. Biometrics 27,
707 857–871. doi:10.2307/2528823

708 Jari Oksanen, Blanchet, F.G., Kindt, R., Legendre, P., Minchin, P.R., O’Hara, R.B., Simpson, G.L.,
709 Solymos, P., Stevens, M.H.H., Wagner, H., 2016. vegan: Community Ecology Package.

710 Maritan, L., Angelini, I., Artioli, G., Mazzoli, C., Saracino, M., 2009. Secondary phosphates in the

- 711 ceramic materials from Frattesina (Rovigo, North-Eastern Italy). *J. Cult. Herit.* 10, 144–
712 151. doi:10.1016/J.CULHER.2008.01.008
- 713 Maritan, L., Mazzoli, C., 2004. Phosphates in archaeological finds: implications for
714 environmental conditions of burial. *Archaeometry* 46, 673–683. doi:10.1111/j.1475-
715 4754.2004.00182.x
- 716 Martín-Fernández, J.A., Buxeda i Garrigós, J., Pawlowsky-Glahn, V., 2015. Logratio analysis in
717 archeometry: principles and methods, in: Barceló, J.A., Bogdanovic, I. (Eds.), *Mathematics*
718 *and Archaeology*. CRC press, Boca Raton FL, pp. 178–189.
- 719 Martínez Ferreras, V., 2015. La difusión comercial de las ánforas vinarias de Hispania Citerior-
720 Tarraconensis (s. I a.C. - I d.C.). *Roman Archaeology* 4. Archaeopress, Oxford.
- 721 Martínez Ferreras, V., 2014. Ánforas vinarias de Hispania Citerior-Tarraconensis (s. I a.C. - I
722 d.C.). Caracterización arqueométrica. *Roman and Late Antique Mediterranean Pottery* 4.
723 Archaeopress, Oxford.
- 724 Martínez Ferreras, V., Capelli, C., Cabella, R., Nieto Prieto, X., 2013. From Hispania
725 Tarraconensis (NE Spain) to Gallia Narbonensis (S France). New data on Pascual 1
726 amphora trade in the Augustan period. *Appl. Clay Sci.* 82, 70–78.
727 doi:10.1016/j.clay.2013.06.021
- 728 Martínez Ferreras, V., Capelli, C., Jézégou, M.-P., Salvat, M., Castellvi, G., Cabella, R., 2015. The
729 Port-Vendres 4 Shipwreck Cargo: evidence of the Roman wine trade in the western
730 Mediterranean. *Int. J. Naut. Archaeol.* 44, 277–299. doi:10.1111/1095-9270.12109
- 731 Marwick, B., 2017. Computational Reproducibility in Archaeological Research: Basic Principles
732 and a Case Study of Their Implementation. *J. Archaeol. Method Theory* 24, 424–450.
733 doi:10.1007/s10816-015-9272-9
- 734 Matthew, A.J., Woods, A.J., Oliver, C., 1991. Spots before the eyes: New comparison charts for
735 visual percentage estimation in archaeological material, in: Middleton, A., Freestone, I.
736 (Eds.), *Recent Developments in Ceramic Petrology*. British Museum, London, pp. 245–59.
- 737 Miró, J., 1988. La producción de ánforas romanas en Catalunya. Un estudio sobre el comercio
738 del vino de la Tarraconense (siglos I a.C.-I d.C.). *BAR International Series* 473, Oxford.
- 739 Ownby, M.F., Huntley, D.L., Peeples, M.A., 2014. A combined approach: using NAA and
740 petrography to examine ceramic production and exchange in the American southwest. *J.*

- 741 Archaeol. Sci. 52, 152–162. doi:10.1016/j.jas.2014.08.018
- 742 Palarea-Albaladejo, J., Martín-Fernández, J.A., 2015. zCompositions -- R package for
743 multivariate imputation of left-censored data under a compositional approach. Chemom.
744 Intell. Lab. Syst. 143, 85--96.
- 745 Pavoine, S., Vallet, J., Dufour, A.-B., Gachet, S., Daniel, H., 2009. On the challenge of treating
746 various types of variables: application for improving the measurement of functional
747 diversity. Oikos 118, 391–402. doi:10.1111/j.1600-0706.2008.16668.x
- 748 Pawlowsky-Glahn, V., Buccianti, A., 2011. Compositional data analysis : theory and
749 applications. Wiley.
- 750 Podani, J., 1999. Extending Gower's General Coefficient of Similarity to Ordinal Characters on
751 JSTOR. Taxon 48, 331–340. doi:10.2307/1224438
- 752 R Core Team, 2015. R: A language and environment for statistical computing.
- 753 Schiffer, M.B., Skibo, J.M., 1997. The Explanation of Artifact Variability. Am. Antiq. 62, 27–50.
754 doi:10.2307/282378
- 755 Schiffer, M.B., Skibo, J.M., 1987. Theory and Experiment in the Study of Technological Change.
756 Curr. Anthropol. 28, 595–622. doi:10.1086/203601
- 757 Schwedt, A., Mommsen, H., Zacharias, N., Buxeda i Garrigós, J., 2006. Analcime crystallization
758 and compositional profiles-comparing approaches to detect post-depositional alterations
759 in archaeological pottery. Archaeometry 48, 237–251. doi:10.1111/j.1475-
760 4754.2006.00254.x
- 761 Sillar, B., Tite, M.S., 2000. The Challenge of “Technological Choices” for Materials Science
762 Approaches in Archaeology. Archaeometry 42, 2–20. doi:10.1111/j.1475-
763 4754.2000.tb00863.x
- 764 Templ, M., Hron, K., Filzmoser, P., 2011. robCompositions: an R-package for robust statistical
765 analysis of compositional data, in: Pawlowsky-Glahn, V. (Ed.), Compositional Data
766 Analysis: Theory and Applications. John Wiley and Sons, pp. 341--355.
- 767 Tite, M.S., 2008. Ceramic Production, Provenance and Use—A Review. Archaeometry 50, 216–
768 231. doi:10.1111/j.1475-4754.2008.00391.x
- 769 van den Boogaart, K.G., Tolosana, R., Bren, M., 2014. compositions: Compositional Data

- 770 Analysis.
- 771 Vila Socias, L., 2011. Una Arqueometria del Canvi Tecnològic: producció i consum d'àmfores
772 durant el canvi d'Era en la zona nord de la costa catalana. Universitat de Barcelona.
- 773 Vila Socias, L., Martínez Ferreras, V., 2015. Caracterización arqueométrica de las ánforas
774 romanas del Collet de Sant Antoni de Calonge, in: La Alfarería Romana Del Collet Est
775 (Calonge, Girona). BAR International Series 2770, Oxford, pp. 211–24.
- 776 Vila Socias, L., Martínez Ferreras, V., Buxeda i Garrigós, J., Kilikoglou, V., 2009. Differences in
777 technological and functional models of contemporary amphorae production in
778 neighbouring areas, in: Proceedings of the 36th International Symposium of
779 Archeometrie (ISA 2006). Québec, pp. 253–59.
- 780 Whitbread, I.K., 1995. Greek transport amphorae: a petrological and archaeological study,
781 Fitch Labo. ed. British School at Athens, Athens.
- 782
- 783